

Evidence for competition between the superconducting and the pseudogap state in $(\text{BiPb})_2(\text{SrLa})_2\text{CuO}_{6+\delta}$ from muon-spin rotation experiments

R. Khasanov,^{1,2,*} Takeshi Kondo,^{3,4} S. Strässle,² D.O.G. Heron,⁵
A. Kaminski,³ H. Keller,² S.L. Lee,⁵ and Tsunehiro Takeuchi^{4,6}

¹Laboratory for Muon Spin Spectroscopy, Paul Scherrer Institut, CH-5232 Villigen PSI, Switzerland

²Physik-Institut der Universität Zürich, Winterthurerstrasse 190, CH-8057 Zürich, Switzerland

³Ames Laboratory and Department of Physics and Astronomy, Iowa State University, Ames, IA 50011, USA

⁴Department of Crystalline Materials Science, Nagoya University, Nagoya 464-8603, Japan

⁵School of Physics and Astronomy, University of St. Andrews, Fife, KY16 9SS, UK

⁶EcoTopia Science Institute, Nagoya University, Nagoya 464-8603, Japan

The in-plane magnetic penetration depth λ_{ab} in optimally doped $(\text{BiPb})_2(\text{SrLa})_2\text{CuO}_{6+\delta}$ (OP Bi2201) was studied by means of muon-spin rotation. The measurements of $\lambda_{ab}^{-2}(T)$ are inconsistent with a simple model of a d -wave order parameter and a uniform quasiparticle weight around the Fermi surface. The data are well described assuming the angular gap symmetry obtained in ARPES experiments [Phys. Rev. Lett **98**, 267004 (2007)], where it was shown that the superconducting gap in OP Bi2201 exists only in segments of the Fermi surface near the nodes. We find that the remaining parts of the Fermi surface, which are strongly affected by the pseudogap state, do not contribute significantly to the superconducting condensate. Our data provide evidence that high temperature superconductivity and pseudogap behavior in cuprates are competing phenomena.

PACS numbers: 74.72.Hs, 74.25.Jb, 76.75.+i

The relevance of the pseudogap phenomenon for superconductivity is an important open issue in the physics of high-temperature cuprate superconductors (HTS's). There are two main scenarios to be considered. In the first, the so-called "precursor scenario", the Cooper pairs are already formed at T^* , the temperature at which the pseudogap opens first, but long-range phase coherence is not established until the sample is cooled below the superconducting transition temperature T_c . In the second, the so-called "two-gap" scenario, the superconducting and the pseudogap state are not directly related with each other, and may even compete. Within this scenario the gaps in k -space, existing near the nodes and in the antinodal region of the Fermi surface, are due to the superconducting and the pseudogap states, respectively. This scenario gained support due to a number of recent experiments [1, 2, 3, 4, 5] which revealed that the antinodal gap remains unaffected as the temperature changes across T_c , and generally its magnitude increases significantly in the underdoped region, where T_c decreases. In contrast, the gap near the nodes scales with T_c and obeys a well defined BCS temperature dependence [4]. This interpretation also agrees with recent results from scanning-tunneling-microscopy experiments of Hanaguri *et al.* [6], suggesting that the incoherent antinodal states are not responsible for the formation of phase-coherent Cooper pairs. Consequently, superconductivity is caused by the coherent part of the Fermi surface near the nodes.

Measurements of the magnetic penetration depth λ can be used to distinguish between the above described scenarios. The temperature dependence of λ is uniquely determined by the absolute maximum value of the superconducting energy gap and its angular and temperature

dependence. In addition, within the London model λ^{-2} is proportional to the superfluid density via $\lambda^{-2} \propto \rho_s \propto n_s/m^*$ and, in case where the supercarrier mass m^* is known, gives information on the supercarrier density n_s .

Here we report on a study of the in-plane magnetic penetration depth λ_{ab} in optimally doped $(\text{BiPb})_2(\text{SrLa})_2\text{CuO}_{6+\delta}$ (OP Bi2201). The angular dependence of the energy gap in similar OP Bi2201 samples was recently studied by Kondo *et al.* [3] by means of angular-resolved photoemission (ARPES), where the observation of two spectral gaps that dominate different regions of the Fermi surface is reported. Our results reveal that $\lambda_{ab}^{-2}(T)$ is inconsistent with a model in which both of these spectral gaps are related to superconductivity, as well as with a superconducting gap of d -wave symmetry developed within the whole Fermi surface. Good agreement with the ARPES data was obtained within a model which assumes that the pseudogap affects the spectral density of the antinodal quasiparticles. Consequently, only carriers close to the nodes contribute to the superfluid density, while the weight of the coherent quasiparticle near the antinodes is negligible. This statement is also supported by comparing the zero-temperature value of $\lambda_{ab}^{-2}(0)$ for OP Bi2201 studied here with those of other OP HTS's, such as $\text{Ca}_{2-x}\text{Na}_x\text{CuO}_2\text{Cl}_2$ (OP Na-CCOC) [7] and $\text{La}_{2-x}\text{Sr}_x\text{CuO}_4$ (OP La214) [8], having similar transition temperatures. It was observed that in superconductors where the superconducting gap is developed only close to the nodes (OP Bi2201 and OP Na-CCOC) the superfluid density is more than 50% smaller than in OP La214 where the d -wave superconducting gap is detected on the whole Fermi surface [9].

Details on the sample preparation for OP Bi2201 sin-

gle crystals can be found elsewhere [10]. The values of T_c and the width of the superconducting transition, as determined from magnetization measurements, are $\simeq 35$ K and $\simeq 3$ K, respectively. The transverse-field muon-spin rotation (TF- μ SR) experiments were performed at the π M3 beam line at the Paul Scherrer Institute (Villigen, Switzerland). Two OP Bi2201 single crystals with an approximate size of $4 \times 2 \times 0.1$ mm³ were mounted on a holder specially designed to perform μ SR experiments on thin single crystalline samples. The sample was field cooled from above T_c to 1.6 K in a series of fields ranging from 5 mT to 640 mT. The magnetic field was applied parallel to the crystallographic c axis and transverse to the muon-spin polarization.

In the TF geometry the local magnetic field distribution $P(B)$ inside a superconductor in the mixed state, probed by means of μ SR, is determined by the coherence length ξ , and the penetration depth λ . In extreme type-II superconductors ($\lambda \gg \xi$) the $P(B)$ distribution is almost independent of ξ and the second moment of $P(B)$ becomes proportional to $1/\lambda^4$ [11]. To describe the asymmetric $P(B)$ (see Fig. 1), the μ SR time spectra were analyzed by using a two-component Gaussian expression [12]. The second moment of $P(B)$ was further obtained as [12]:

$$\langle \Delta B^2 \rangle = \frac{\sigma^2}{\gamma_\mu^2} = \sum_{i=1}^2 \frac{A_i}{A_1 + A_2} \left[\frac{\sigma_i^2}{\gamma_\mu^2} + \left(B_i - \frac{A_i B_i}{A_1 + A_2} \right)^2 \right]. \quad (1)$$

Here A_i , σ_i , and B_i are the asymmetry, the relaxation rate, and the mean field of the i -th component, and $\gamma_\mu = 2\pi \times 135.5342$ MHz/T is the muon gyromagnetic ratio. The analysis was simplified to a single Gaussian lineshape in the case when the two-Gaussian and the one-Gaussian fits result in comparable χ^2 . The superconducting part of the second moment σ_{sc}^2 was obtained by subtracting the contribution of the nuclear moments σ_{nm} measured at $T > T_c$ as $\sigma_{sc}^2 = \sigma^2 - \sigma_{nm}^2$ [12]. Since the magnetic field was applied along the crystallographic c axis, our experiments provide direct information on λ_{ab} .

Fig. 1a shows the dependence of σ_{sc} on the applied magnetic field measured after field cooling the OP Bi2201 sample from $T > T_c$ down to 1.6 K. The $P(B)$ distributions were calculated using the maximum entropy Fourier-transform technique for $\mu_0 H = 5$ mT, 40 mT, and 640 mT (see Fig. 1a). In the whole range of fields ($5 \text{ mT} \leq \mu_0 H \leq 640 \text{ mT}$) $P(B)$ is asymmetric. The asymmetric shape of $P(B)$ is generally described in terms of the so-called skewness parameter $\alpha_s = \langle \Delta B^3 \rangle^{1/3} / \langle \Delta B^2 \rangle^{1/2}$ [$\langle \Delta B^n \rangle$ is the n -th central moment of $P(B)$]. α_s is a dimensionless measure of the asymmetry of the lineshape, the variation of which reflects underlying changes in the vortex structure [14]. In the limit $\kappa \gg 1$ and for realistic measuring conditions $\alpha_s \simeq 1.2$ for an ideal triangular vortex lattice (VL). It is very sensitive to structural changes of the VL which

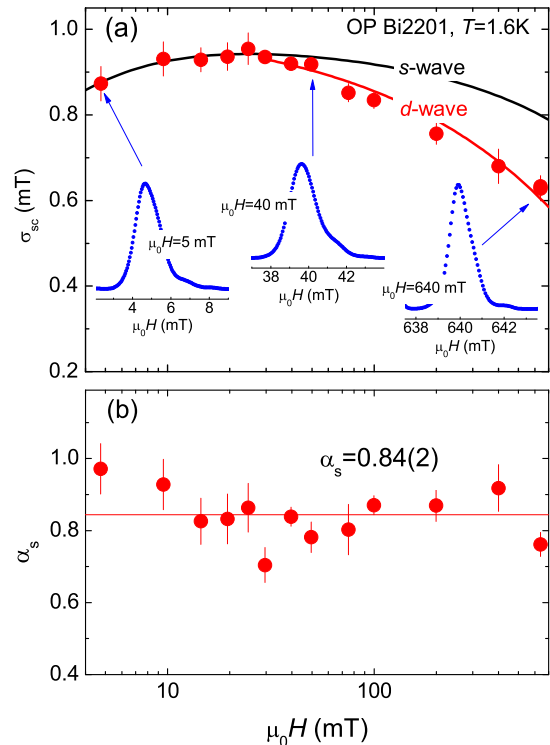


FIG. 1: (Color online) (a) Dependence of σ_{sc} of OP Bi2201 on the applied magnetic field measured at $T = 1.6$ K. The black solid line corresponds to $\sigma_{sc}(H)$ obtained by using the numerical calculations of Brandt [11] ($\lambda = 360$ nm, $\kappa = 140$) for a superconductor with an isotropic energy gap. The solid red line represents $\sigma_{sc}(H)$ expected in case of a d -wave superconductor. The blue dotted curves show the local magnetic field distribution $P(B)$ calculated by means of the maximum entropy Fourier-transform technique at $T = 1.6$ K and $\mu_0 H = 5$ mT, 40 mT, and 640 mT. (b) Field dependence of the skewness parameter α_s . The solid line is the average value $\alpha_s = 0.84(2)$.

can occur as a function of temperature and/or magnetic field [14, 15]. Fig. 1b implies that in OP Bi2201 $\alpha_s(H)$ is almost constant [$\alpha_s = 0.84(2)$] and is smaller than the expected value of 1.2, which is probably caused by distortions of the VL due to pinning effects. It is known that Pb substitution in double-layer Bi2212 HTS's enhances pinning quite substantially [13].

It should be noted here that addition of Pb does not change T_c and the in-plane superfluid density $\rho_s \propto \lambda_{ab}^{-2}$ [16], but makes OP Bi2201 *more* 3-dimensional. To estimate the anisotropy coefficient $\gamma_{c,ab} = \lambda_c / \lambda_{ab}$ (λ_c is the c -axis component of the penetration depth) we performed torque magnetization experiment on one of the crystals studied [17]. A value of $\gamma_{c,ab} \simeq 20$ was found, which is more than 10 times smaller than $\gamma_{c,ab} \simeq 200 - 400$ obtained on OP Bi2201 without Pb by Kawamura *et al.* [18].

Figure 1 indicates that the magnetic field dependence

of σ_{sc} is not monotonic: with increasing field σ_{sc} goes through the broad maximum at around 20 mT. The black solid line in Fig. 1a, calculated within the model of Brandt [11], corresponds to $\sigma_{sc}(H)$ for an isotropic s -wave superconductor with $\lambda = 360$ nm and $\kappa = \lambda/\xi \simeq 140$ ($\xi \simeq 2.6$ nm was obtained from the value of the second critical field $\mu_0 H_{c2}(0) \simeq 50$ T [19]). From Fig. 1a we conclude that the experimental $\sigma_{sc}(H)$ depends much stronger on the magnetic field than expected for a fully gaped s -wave superconductor. As shown by Amin *et al.* [20] for a superconductor with nodes in the energy gap a field dependent correction to ρ_s arises from its nonlocal and nonlinear response to an applied magnetic field. The solid red line represents the result of the fit by means of the relation:

$$\frac{\rho_s(H)}{\rho_s(H=0)} = \frac{\sigma_{sc}(H)}{\sigma_{sc}(H=0)} = 1 - K\sqrt{H}, \quad (2)$$

which takes the nonlinear correction to ρ_s for a superconductor with a d -wave energy gap into account [21]. Here the parameter K depends on the strength of the nonlinear effect. Since Eq. (2) is valid for intermediate fields $H_{c1} \ll H \ll H_{c2}$ (H_{c1} is the first critical field) only the data points above 40 mT were considered in the analysis.

We now discuss the T dependence of σ_{sc} . Figure 2 displays $\sigma_{sc}(T)$ measured at $\mu_0 H = 40$ mT. Below 20 K σ_{sc} is linear in T as expected for a superconductor with nodes in the gap, consistent with the conclusion drawn from the analysis of the $\sigma_{sc}(H)$ data (see discussion above and Fig. 1). To ensure that $\sigma_{sc}(T)$ is determined primarily by the variance of the magnetic field within the VL we plot in Fig. 2b the corresponding $\alpha_s(T)$. It is constant from 1.6 K to $\simeq 27$ K and drops to zero at $T \simeq 30$ K, where $P(B)$ becomes fully symmetric. A similarly sharp change of α_s with temperature was observed in Bi2212 and was explained by VL melting [14, 15]. Correspondingly, we conclude that for temperatures $0 < T \lesssim 30$ K the T variation of σ_{sc} reflects the *intrinsic* behavior of the in-plane magnetic penetration depth λ_{ab} .

The T dependence of σ_{sc} was analyzed by assuming that the angular dependence of the energy gap in OP Bi2201 is similar to the one from recent ARPES experiments [3] (see Fig. 3a). In analogy with Refs. 3 and 4 it was also assumed that the energy gap in the nodal region changes with temperature in accordance with the weak-coupling BCS prediction $\tilde{\Delta}(T/T_c) = \tanh\{1.82[1.018(T_c/T - 1)^{0.51}]\}$ [22], while the one near the antinodes is T independent (see the corresponding lines "A" and "B" in Fig. 3b). The following cases were considered: (I) a monotonic d -wave gap $\Delta(T, \varphi) = 15 \text{ meV} \cdot \cos(2\varphi)\tilde{\Delta}(T/T_c)$ (green dashed line); (II) a monotonic d -wave gap with suppressed quasiparticle weight in the antinodal region (solid orange line); (III) an analytical function, which follows the monotonic d -wave $15 \text{ meV} \cdot \cos(2\varphi)\tilde{\Delta}(T/T_c)$ in the nodal region and changes

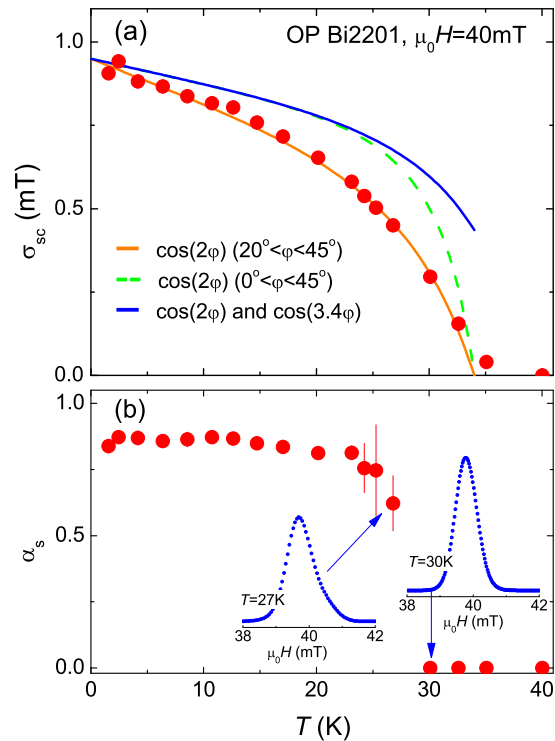


FIG. 2: (Color online) (a) Dependence of σ_{sc} of OP Bi2201 on T measured at $\mu_0 H = 40$ mT. Lines represent the theoretical $\sigma_{sc}(T)$ curves obtained by assuming different symmetries of the superconducting energy gap (see Fig. 3a). (b) Dependence of the skewness parameter α_s on T . The blue dotted curves represent $P(B)$ distributions below ($T = 27$ K) and above ($T = 30$ K) the VL melting temperature.

to a $36 \text{ meV} \cdot \cos(3.4\varphi)$ behavior close to the antinodes (solid blue line). The T dependence of the magnetic penetration depth was calculated within the local (London) approximation ($\lambda \gg \xi$) using the following equation [23]:

$$\frac{\sigma_{sc}(T)}{\sigma_{sc}(0)} = 1 + \frac{8}{\pi - 4\varphi_0} \int_{\varphi_0}^{\pi/4} \int_{\Delta(T, \varphi)}^{\infty} \left(\frac{\partial f}{\partial E} \right) \frac{E dE d\varphi}{\sqrt{E^2 - \Delta(T, \varphi)^2}}. \quad (3)$$

$f = [1 + \exp(E/k_B T)]^{-1}$ denotes the Fermi function. Here we also replace the prefactor $8/\pi$ of the integral with $8/(\pi - 4\varphi_0)$ to account for the case when the superconducting energy gap is developed only on a part of the Fermi surface (in our case from φ_0 to $\pi/4$). The results of this analysis are presented in Fig. 2a. The monotonic d -wave gap as well as the combined gap represented by the solid blue line in Fig. 3a can not describe the experimental $\sigma_{sc}(T)$. Full consistency between ARPES and μ SR data is obtained if one assumes a superconducting d -wave gap with only carriers in the region $20^\circ \lesssim \varphi < 45^\circ$ contributing to the superfluid. It should be noted here that the theoretical $\sigma_{sc}(T)$ curves in Fig. 2 were not fitted, but obtained directly by introducing the angular dependence of the gap measured in ARPES ex-

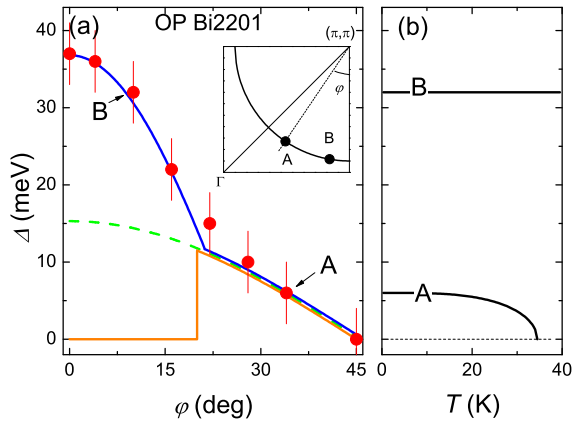


FIG. 3: (Color online) (a) Angular dependence of the energy gap of OP Bi2201 obtained in ARPES experiments [3]. Lines represent the various models of the gap symmetries used to analyze the experimental $\sigma_{sc}(T)$ data (see Fig. 2a). The inset shows schematically a part of the Fermi surface. The points "A" and "B" are close to the nodal ($\varphi \sim 45^\circ$) and the antinodal ($\varphi \sim 0^\circ$) region, respectively. (b) Temperature dependence of the energy gap in the nodal (curve A) and the antinodal (curve B) regions.

periments into Eq. (3), describing the T dependence of the penetration depth within the London approach.

TABLE I: Transition temperature T_c , zero-temperature in-plane magnetic penetration depth $\lambda_{ab}^{-2}(0)$, and angular region where the superconducting d -wave gap is observed for OP Bi2201 (studied here), OP Na-CCOC, and OP La214.

Compound	T_c (K)	$\lambda_{ab}^{-2}(0)$ (μm^{-2})	SC gap region
OP Bi2201	35	7.8	$20^\circ \lesssim \varphi < 45^\circ$ ^(a)
OP Na-CCOC	28	10.0	$20^\circ \lesssim \varphi < 45^\circ$ ^(c)
OP La214	36	15.0	$0^\circ \leq \varphi < 45^\circ$ ^(e)

^(a) Ref. 3, ^(b) Ref. 7, ^(c) Ref. 6, ^(d) Ref. 8, ^(e) Ref. 9

Next we compare the zero-temperature values of $\lambda_{ab}^{-2}(0) \propto n_s/m^*$ for various OP HTS's having comparable T_c values and for which the angular dependence of the superconducting gap was measured [3, 6, 9]. OP La214, which exhibits a fully developed superconducting gap, has an approximately 50% higher value of the superfluid density as compared to both OP Na-CCOC and OP Bi2201, having the superconducting gap opened only on a limited part of the Fermi surface (see Table I). Assuming that the supercarrier masses m^* are the same for all OP compounds listed in Table I (in analogy with $m^* \simeq 3 - 4m_e$ reported for La214 and $\text{YBa}_2\text{Cu}_3\text{O}_{7-\delta}$ families of HTS's [24]), the difference in the values of $\lambda_{ab}^{-2}(0)$ can be naturally explained by the different number of carriers condensed into the superfluid. In the case of OP Bi2201 and OP Na-CCOC, n_s is strongly reduced

because of the fraction of the states is no more available for the superconducting condensate due to the pseudogap.

To conclude, the in-plane magnetic penetration depth λ_{ab} in optimally doped Bi2201 was studied by means of muon-spin rotation. By comparing the measured $\lambda_{ab}^{-2}(T)$ with the one calculated theoretically using a model consistent with ARPES measurement [3] we found that the superconducting gap in OP Bi2201 has d -wave symmetry, but only carriers from parts of the Fermi surface close to the node ($20^\circ \lesssim \varphi \lesssim 45^\circ$) contribute to the superfluid. This implies that the pseudogap affects the spectral density of the quasiparticles and, consequently, not all the states at the Fermi surface are available to participate in the superconducting condensate. Our results supports the scenario where the superconducting and pseudogap state are two distinct and competing phenomena. This statement is also consistent with the fact that the superfluid density in OP Bi2201 is strongly reduced in comparison with that in OP La214, where the superconducting gap and coherent quasiparticles are observed along the whole Fermi surface ($0^\circ \leq \varphi < 45^\circ$) [9].

This work was performed at the Swiss Muon Source (S μ S), Paul Scherrer Institute (PSI, Switzerland). The authors are grateful to Y.J. Uemura and R. Prozorov for stimulating discussions, and S. Weyeneth for performing torque experiments. This work was supported by the K. Alex Müller Foundation and in part by the Swiss National Science Foundation. Work at the Ames Laboratory was supported by the Department of Energy - Basic Energy Sciences under Contract No. DE-AC02-07CH11358.

* Electronic address: rustem.khasanov@psi.ch

- [1] M. Le Tacon *et al.*, Nature Physics **2**, 537 (2006).
- [2] K. Tanaka *et al.*, Science **314**, 1910 (2006).
- [3] T. Kondo *et al.*, Phys. Rev. Lett. **98**, 267004 (2007).
- [4] W.S. Lee *et al.*, Nature (London) **450**, 81 (2007).
- [5] W. Guyard *et al.*, Phys. Rev. B **77**, 024524 (2008).
- [6] T. Hanaguri *et al.*, Nature Physics **3**, 865 (2007).
- [7] R. Khasanov *et al.*, Phys. Rev. B **76**, 094505 (2007).
- [8] C. Panagopoulos *et al.*, Phys. Rev. B **60**, 14617 (1999).
- [9] M. Shi *et al.*, unpublished, arXiv:0708.2333.
- [10] T. Kondo *et al.*, J. Electron Spectrosc. Relat. Phenom. **137-140**, 663 (2004); T. Kondo *et al.*, Phys. Rev. B **72**, 024533 (2005).
- [11] E.H. Brandt, Phys. Rev. B **68**, 054506 (2003).
- [12] R. Khasanov *et al.*, Phys. Rev. B **73**, 214528 (2006).
- [13] N. Musolino *et al.*, Physica C **399**, 1 (2003).
- [14] S.L. Lee *et al.*, Phys. Rev. Lett. **71**, 3862 (1993).
- [15] C.M. Aegerter *et al.*, Phys. Rev. B **57**, 1253 (1998).
- [16] P.L. Russo *et al.*, Phys. Rev. B **75**, 054511 (2007).
- [17] S. Weyeneth, under preparation.
- [18] S. Kawamata *et al.*, J. Low. Temp. Phys. **117**, 891 (1999).
- [19] Y. Wang *et al.*, Science **299**, 86 (2003).
- [20] M.H.S. Amin, M. Franz, and I. Affleck, Phys. Rev. Lett.

- 84**, 5864 (2000).
- [21] I. Vekhter, J.P. Carbotte, and E.J. Nicol, Phys. Rev. B **59**, 1417 (1999).
- [22] A. Carrington and F. Manzano, Physica C **385**, 205 (2003).
- [23] R. Khasanov *et al.*, Phys. Rev. Lett. **98**, 057007 (2007).
- [24] W.J. Padilla *et al.*, Phys. Rev. B **72**, 060511 (2005).